Oscillatory NAD(P)H Waves and Calcium Oscillations in Neutrophils? A Modeling Study of Feasibility

Oliver Slaby and Dirk Lebiedz*
Center for Systems Biology, Freiburg, Germany

ABSTRACT The group of Howard Petty has claimed exotic metabolic wave phenomena together with mutually phase-coupled NAD(P)H- and calcium-oscillations in human neutrophils. At least parts of these phenomena are highly doubtful due to extensive failure of reproducibility by several other groups and hints that unreliable data from the Petty lab are involved in publications concerning circular calcium waves. The aim of our theoretical spatiotemporal modeling approach is to propose a possible and plausible biochemical mechanism which would, in principle, be able to explain metabolic oscillations and wave phenomena in neutrophils. Our modeling suggests the possibility of a calcium-controlled glucose influx as a driving force of metabolic oscillations and a potential role of polarized cell geometry and differential enzyme distribution for various NAD(P)H wave phenomena. The modeling results are supposed to stimulate further controversial discussions of such phenomena and potential mechanisms and experimental efforts to finally clarify the existence and biochemical basis of any kind of temporal and spatiotemporal patterns of calcium signals and metabolic dynamics in human neutrophils. Independent of Petty's observations, they present a general feasibility study of such phenomena in cells.

INTRODUCTION

Human immune cells are classified into different types according to their functions in adaptive and innate immunity (1). Whereas cells of adaptive immunity respond in an antigen-specific way to invading pathogens, cells of innate immunity recognize molecular components that are conserved among a large group of microorganisms.

An important cell type of innate immunity is the neutrophil, a terminally differentiated peripheral blood cell (2). Neutrophils are part of the first line of defense against microorganisms and usually circulate in the blood stream. They leave the vascular system at a location of tissue inflammation after becoming adherent to the vessel wall acquiring a flat elongated and polarized shape and chemotactically migrate toward the focus of inflammation within the extracellular matrix. After recognition by cell surface receptors, the pathogens are engulfed via phagocytosis and killed by phagolysosome formation and production of reactive oxygen metabolites.

Recently, Petty et al. claimed the observation of self-organized patterns in terms of spatiotemporal NAD(P)H, which denotes the sum of nicotinamide adenine dinucleotide (NADH) and nicotinamide adenine dinucleotide phosphate-oxidase (NADPH), concentration waves in neutrophils using fluorescence microscopy (3,4). In addition to these waves, sinusoidal temporal oscillations of NAD(P)H with periods of 20 and 10 s have been detected by fluorimetric whole-cell measurements of NAD(P)H autofluorescence (5).

Interestingly, Petty et al. have observed similar oscillatory properties for Ca^{2+} signals. They observe that calcium spikes occur with the same frequency and a constant phase relation to NAD(P)H (5). Both oscillators consistently show an increase in frequency from ~20s to a 10 s period after activation of neutrophils with proinflammatory stimuli like fMLP or cytokines (6,7) while retaining their phase locking.

In addition to the oscillations, ''high-speed-fluorescence-microscopy'' (8) results from the Petty group show NAD(P)H-waves in the nonactivated state being ignited exclusively at the rear of the cell (uropod) propagating unidirectionally toward the front (lamellipodium) with a velocity of ~15–50 μm/s (see Fig. 1 and (3,4,9)). Each wave is annihilated after reaching the cell front and a new wave starts at the rear. After proinflammatory stimulation, two NAD(P)H waves are observed propagating in opposite directions. These are reflected at the front and the rear end of the cell, respectively, and do not affect each other when colliding in the middle of the cell body.

Further high-speed imaging observations by the Petty group suggest that oscillatory calcium spikes also correspond to spatiotemporal events. During each spike, a submembrane calcium wave with a velocity of ~150–180 μm/s starts at the lamellipodium, propagates around the perimeter of the cell, and is annihilated after returning to the lamellipodium (10). However, the existence of such waves is highly doubtful because of extensive failure to reproduce them (11,12) and (M. M. Davis and A. Weiss, Howard Hughes Medical Institute, personal communication, 2008).

The direction of cell polarization and migration seems to correspond to the direction of NAD(P)H wave propagation, which is perturbed on the timescale of milliseconds after asymmetric application of a chemoattractant locally to the cell membrane perpendicular to the original direction of wave propagation (3). The wave direction is then quickly adjusted toward the site of attractant binding to cell surface

Submitted June 25, 2008, and accepted for publication September 29, 2008.

*Correspondence: dirk.lebiedz@biologie.uni-freiburg.de

Editor: Jason M. Haugh.

0006-3495/09/01/0417/12 $2.00

doi: 10.1016/j.bpj.2008.09.044

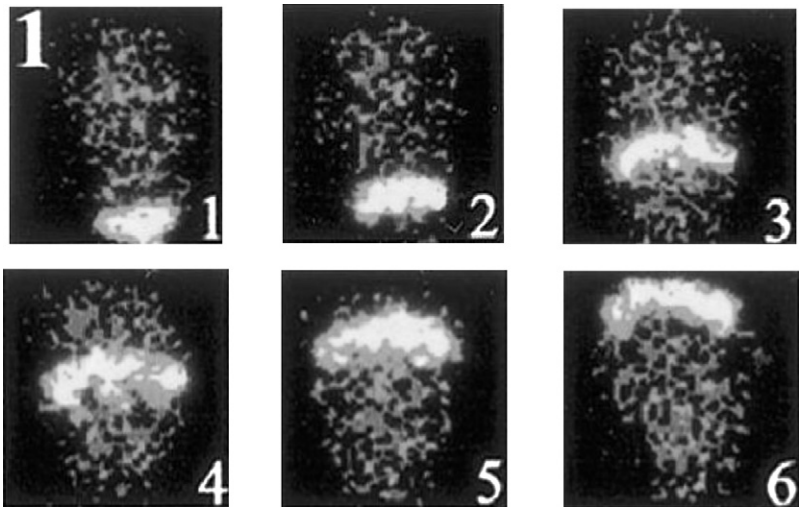

FIGURE 1 Spatiotemporal measurements of NAD(P)H wave propagation using high speed microscopy in adherent polarized neutrophils. A time series of NAD(P)H fluorescence images is shown. The cell leading edge of the cell is oriented toward the top of each frame, the uropod is near the bottom. Time interval of 100-ms interval between micrographs. (Image taken with permission from Petty and Kindzelskii (3), where it appears in color. Copyright (2001) National Academy of Sciences, Washington, DC.)

receptors. Therefore, possible directional wave propagation in neutrophils might be interpreted as a potential signaling mechanism involved in direction finding issues during chemotactic movement. In general, mechanisms for the transfer of extracellular anisotropic information into asymmetric intracellular patterns could be central for spatial signal processing.

The described exotic-wave phenomena are mechanistically unclear; however, provided phenomena of that type exist, they might represent an important signaling route used by the cell to translate spatially nonuniform extracellular signals like chemoattractant concentration gradients into asymmetric intracellular signals.

To stimulate an effort for full elucidation, we use mathematical modeling to analyze a potential underlying mechanism, which, in principle, could explain the observed spatiotemporal patterns and would have to be experimentally validated. In particular, we shed some light on the potential phase coupling between calcium signaling and metabolic dynamics. We highlight the importance of an integrative modeling approach taking into account experimental data from both purely temporal and spatiotemporal measurements and explaining a variety of dynamic phenomena simultaneously at the system level. This is at the core of systems biology research and a fundamental understanding of signaling and metabolic dynamics needs studies in both space and time. Modeling with ordinary differential equations (ODE) assuming a continuously stirred spatially homogeneous reactor is not sufficient for the system studied here, because the resulting phenomena Petty et al. claim, e.g., oscillations, regarded from a purely temporal perspective in a whole cell average, would have to be mechanistically consistent with the observed spatiotemporal dynamics. Therefore, we develop for the first time an integrated spatiotemporal modeling framework for complex wave propagation and oscillation phenomena observed by Petty in neutrophils and show how such phenomena, waves and oscillations, could in principle be mechanistically explained. Our results demonstrate that, assuming the wave phenomena are real, an ODE model for the NAD(P)H oscillations published recently (13) is inadequate and has to be modified and extended to a spatial model for a systems approach to the phenomena. This is because it neither attempts to describe the coupling between calcium and metabolism nor the simultaneous existence of NAD(P)H oscillations and spatial waves observed by Petty. Our spatiotemporal model can explain both aspects consistently. It is of reaction-diffusion type and based on glycolysis which is known to be the main metabolic energy source of neutrophils. The main modeling result is that NAD(P)H waves could arise from glycolysis and the NAD(P)H oscillations might be driven by calcium-controlled glucose influx feedback-coupled to metabolism via cyclic ADP ribose (cADPR) synthesis from NAD^+ and cADPR-gated calcium entry from intracellular stores.

Based on the assumption of glucose influx control by calcium we provide a plausible mechanism potentially explaining unidirectional wave propagation by geometric considerations in accordance with the morphology of a polarized neutrophil. Finally, we present a potential explanation for wave crossing and boundary reflection behavior based on a heterogeneous glycolytic enzyme distribution found experimentally. We underpin all our hypotheses with evidence from published experimental findings in the context of metabolic regulation and its relation to calcium signaling in activated and nonactivated neutrophils. All modeling results and hypotheses we derive are largely consistent with experimental knowledge published so far for the system under study and are capable of explaining spatiotemporal metabolic dynamics of the type observed in high-speed imaging experiments by the Petty group, which are, however, highly controversial. Our modeling study calls for a final experimental clarification by the scientific community of the existence and a mechanistic elucidation of any kind of such dynamic phenomena claimed by Petty et al.

MODELING

Kinetic modeling of glycolysis and calcium signaling

It has been discussed in the literature that the main energy source of neutrophils is anaerobic glycolysis (14). Studies from the Petty group using metabolic inhibitors show disappearance of NAD(P)H autofluorescence waves (3). Therefore, we rely on modeling the upper part of glycolysis according to the model by Kummer et al. (13). Our model is based on that of Kummer et al., with some crucial modifications and extensions that will be pointed out below.

Increased hexose-monophosphate-shunt (HMS) activity after proinflammatory stimulation of neutrophils has been found, and its contribution to metabolic dynamics in particular, in the activated state, has been confirmed in inhibitor studies (15). As in Kummer et al. (13), we use a simple linear first-order rate expression $k_{\mathrm{hms}}[\mathrm{G6P}]$ modeling the consumption of glucose-6-phosphate in the HMS and the corresponding NADPH production. NADPH contributes strongly (~50%) to the NAD(p)H signal, when simulating an activated state of the neutrophil. In simulation results considering the nonactivated states, NADPH contributes only less (~1%) to the signal.

The reactions catalyzed by hexokinase (HK) and fructose-bisphosphate aldolase (FBA) are modeled using one-substrate Michaelis-Menten terms. The glyceraldehyde-3-phosphate-dehydrogenase (GAPDH) step is modeled by Michaelis-Menten kinetics for two substrates; irreversibility and a constant concentration of phosphate are assumed, which are strong but reasonable simplifications, because the GAPDH-reaction has only a limited influence on the overall system dynamics, as shown in Kummer et al. (13). We assume a constant total concentration of the sum of NADH and its oxidized form NAD^+ incorporating mass conservation of $[\mathrm{NADH}]+[\mathrm{NAD}^+]$ into the model. For both NADH and NADPH, the simple linear reaction terms $k_{\mathrm{NADH}}[\mathrm{NADH}]$ and $k_{\mathrm{NADPH}}[\mathrm{NADPH}]$ are used to model cellular consumption of these metabolites.

The reaction catalyzed by the extensively regulated enzyme phosphofructokinase (PFK) is modeled as in Westermark and Lansner (16), using a term suggested in Hofmeyr and Cornish-Bowden (17) for an irreversible reaction with product activation. In Westermark and Lansner (16), a saturation of phosphofructokinase with respect to adenosine triphosphate is assumed, which is another regulatory metabolite of glycolysis.

In contrast to Kummer et al. (13), we assume fast equilibrium for the glucose-phosphate-isomerase reaction (GPI) as in Westermark and Lansner (16) and model this reaction only implicitly, since it is assumed that the GPI-step is reversible displaying high activity (18,19). The parameter v_{gpi} denotes the corresponding equilibrium conversion constant. In addition to that, we make some changes to parameter values (see Table 3) compared to the Kummer model.

We further include a calcium-signaling module using a qualitative model proposed by Li and Rinzel (20). The model is based on IP_3 channel gating behavior. Using a timescale separation argument, the calcium dynamics can be described involving only two dynamical variables—the intracellular calcium concentration $[Ca^{2+}]$ and the fraction of channels not inactivated by calcium. The calcium flux from the ER into the cytoplasm includes IP_3-induced channel gating, calcium-induced calcium release, and transport of calcium into the ER via SERCA-pumps. This is motivated by the experimental observation that the system seems to play an active role in inflammatory calcium signaling (21–23). Therefore, we focus on this key regulatory step of calcium signaling in neutrophils. Additional calcium fluxes through the plasma membrane may also be involved, but for a qualitative description of intracellular calcium dynamics, we focus on this core mechanism. For a coupling of the calcium model to the glycolysis model, we propose a production of the ryanodine receptor activating substance cyclic ADP ribose (cADPR), which is synthesized from NAD^+, and extend the Li-Rinzel model by an additional calcium influx via ryanodine receptors which are activated by cADPR. Involvement of cADPR in calcium mobilization and its importance for cellular functions like chemotaxis has been demonstrated for neutrophils (24,25). We model cADPR production using mass action kinetics with a production term $k_{\mathrm{cadp}}[\mathrm{NAD}]^+$ and a cellular consumption $k_{\mathrm{cadp_c}}$ [cADPR] and the activation of ryanodine receptors using a Hill-type equation (see Table 2).

The Ca^{2+}-driven glucose influx is modeled using a constant influx ''in'' and a Ca^{2+}-dependent term $V_{\mathrm{in}}[Ca^{2+}]/(K_{\mathrm{in}} + [Ca^{2+}])$. This assumption is motivated by the knowledge that glucose transport in neutrophils is dynamically regulated (26) and the fact that calcium seems to be involved in this regulation (27). Tables 1–5 contain all used reaction terms, corresponding parameter values, and initial conditions, and provide the full differential equation model we used.

TABLE 1 Rate equations for the glycolysis model

Reaction number	Name	Kinetics
R1	HK	$\frac{V_{\mathrm{hk}}[\mathrm{Glc}]}{K_{\mathrm{hk}} + [\mathrm{Glc}]}$
R2	PFK	$\frac{V_{\mathrm{pfk}}[\mathrm{F6P}]^h}{[\mathrm{F6P}]^h + K_{\mathrm{pfk}}^h \frac{(1+(k_x[\mathrm{FBP}])^{h_x})}{1+\alpha^h(k_x[\mathrm{FBP}])^{h_x}}}$ $h = h_{\mathrm{pfk}} - \sigma\frac{[\mathrm{FBP}]}{K_{\mathrm{fba}}+[\mathrm{FBP}]}$
R3	FBA	$\frac{V_{\mathrm{fba}}[\mathrm{FBP}]}{K_{\mathrm{fba}}+[\mathrm{FBP}]}$
R4	GAPDH	$\frac{V_{\mathrm{gapdh}}[\mathrm{GAP}][\mathrm{NAD}^+]}{K_{\mathrm{igap}}K_{\mathrm{nad}}+K_{\mathrm{gap}}[\mathrm{NAD}^+]+K_{\mathrm{nad}}[\mathrm{GAP}]+[\mathrm{GAP}][\mathrm{NAD}^+]}$

Note that HK is glucokinase; PFK is phosphofructokinase; FBA is fructose-bisphosphate aldolase; and GAPDH is glyceraldehyde-3-phosphate-dehydrogenase.

TABLE 2 Rate equations for the calcium model

Reaction number	Species	Kinetics
R5	$[Ca^{2+}]$	$\frac{f_i}{V_i}\left(L + \frac{P_{IP_3R}[IP_3]^3[Ca^{2+}]^3h^3}{([IP_3]+K_i)^3([Ca^{2+}]+K_a)^3} + \frac{V_{RyR}[cADPR]^3}{[cADPR]^3+K_{RyR}^3}\right)$
		$\left([Ca^{2+}_{ER}] - [Ca^{2+}]\right) - \frac{f_i}{V_i}\left(\frac{V_{SERCA}[Ca^{2+}]^2}{[Ca^{2+}]^2+K_{SERCA}^2}\right)$
R6	h	$A(K_d - ([Ca^{2+}] + K_d)h)$
	$[Ca^{2+}_{ER}]$	$\frac{[Ca^{2+}]_T - [Ca^{2+}]}{\sigma_h}$

Spatiotemporal modeling of metabolic dynamics

For modeling the spatiotemporal behavior, we assume a reaction diffusion mechanism

TABLE 3 Parameter values—rate constants for the glycolysis model

Kinetic parameter	Parameter value
V_{hk}	250 μmol/s
v_{GPI}	3.5
K_{pfk}	2000 μmol
h_x	2.5
α	5
σ	1.5
V_{gapdh}	7000 μmol/s
K_{nad}	50 μmol
k_{NADH}	5 s^{-1}
k_{NADPH}	5 s^{-1}
f_i	0.01 pL/s
L	0.37 pL/s
K_i	1 amol
V_{RyR}	16 amol/s
V_{SERCA}	400 amol/s
A	0.8
σ_h	0.185
$[IP_3]$	0.4 μmol
k_{cadp_c}	35 s^{-1}
V_{in}	18 μmol/s
k_{hms}	0.01 s^{-1}
K_{hk}	47 μmol
V_{pfk}	8000 μmol/s
k_x	10
K_{fba}	5 μmol
h_{pfk}	2.5
V_{fba}	400 μmol/s
K_{igap}	3210 μmol
K_{gap}	98 μmol
c_{sum}	5000 μmol
GLC_{in}	100 μmol/s
$\overline{V}_i$	4 pL
P_{IP_3R}	26,640 amol/s
K_a	0.4 amol
K_{RyR}	0.1 amol
K_{SERCA}	0.2 amol
K_d	0.4 amol
Ca^{2+}_T	4 μmol
k_{cadp}	0.003 s^{-1}
in	16 μmol
K_{in}	1 μmol

TABLE 4 General initial conditions for the numerical simulations of the glycolysis model; differing values are given in the article

Species	Initial value
[G6P]	200 μmol
[FBP]	0.01 μmol
[GAP]	10 μmol
[NADH]	10 μmol
[NADPH]	1 μmol
$[Ca^{2+}]$	0.2 μmol
[h]	0.9 μmol
[cADPR]	1 μmol
[GLC]	30 μmol

$$\frac{\partial u}{\partial t} = f_{GLYCO}(u) + D\Delta u \text{ in } \Omega. \quad (1)$$

Here, u denotes the vector of model variables (glycolytic metabolites) according to the kinetic modeling of glycolysis as in Kummer et al. (13) and $f_{GLYCO}(u)$, the corresponding kinetic model described in the previous section. D is a diagonal matrix containing diffusion constants, Ω is the geometric domain describing the neutrophil, and Δu denotes the Laplacian operator.

We assume zero flux von-Neumann boundary conditions for all species except for glucose which is transported into the cell over the plasma membrane,

$$\frac{\partial u}{\partial \vec{n}} = 0 \text{ on } \partial\Omega, \quad (2)$$

where $\partial u/\partial \vec{n}$ denotes the normal derivative to the boundary $\partial\Omega$.

Because we study the effect of glucose influx on the wave and oscillation phenomena, we model it in this case considering unidirectionality of wave propagation based on geometry (see below) explicitly as

$$\frac{\partial [GLC]}{\partial \vec{n}} = GLC_{in} \text{ on } \partial\Omega. \quad (3)$$

In all other scenarios, we consider glucose as (inhomogeneous) parameter (see below) to reduce model dimensions for computation. Values used for corresponding simulations are given in the captions.

TABLE 5 Differential equations of the kinetic model; usage of the corresponding equations is explained in the article

Species	Right-hand side $f(u)$
[GLC]	−R1
[G6P]	R1-R2
[FBP]	R2-R3
[GAP]	2 R3-R4
[NADH]	R4-k_{NADH}[NADH]
[NADPH]	$2\cdot k_{hms}$[G6P] − k_{NADPH}[NADPH]
[cADPR]	$k_{cadp}[NAD^+] - k_{cadp_c}$[cADPR]
$[Ca^{2+}]$	R5
[h]	R6

Discussion of used parameters

Given the fact that the model is rather qualitative or at most semiquantitative in nature because most parameters are undetermined in vivo for neutrophils, Kummer et al. (13) studied the robustness of the model by varying the individual parameter values. They found that many parameters have only limited effect on the model dynamics, and since we use mostly the same parameter values or values which are in the robustness range of their sensitivity analysis, similar robustness is also observed for our model.

For estimation of the unknown diffusion coefficients in living neutrophils, we use the Stokes-Einstein equation (28) for Newtonian fluids as a rough approximation

$$D = \frac{k_B T}{6\pi\eta r} \tag{4}$$

with the Boltzmann constant k_B, absolute temperature T, viscosity η, and particle radius r. Choosing an absolute temperature of 310 K, e.g., 37°C, viscosity of $\eta = 11$ mPa s (29), and an approximated molecular radius $r = 400$ pm for the glycolytic metabolites, we obtain an approximation of the diffusion coefficient of $D \approx 50\mu m^2/s$. The approximated molecular radius is estimated assuming a hexagon and determined calculating the radius of the circle cutting all edges via simple geometric considerations and known length of C-C and C-H bonds (28). This is probably an overestimation, since this value neglects the reversible binding of metabolites to other intracellular components and percolation through the numerous intracellular structures in terms of molecular crowding. Therefore, we assume a diffusion coefficient $D = 2\mu m^2/s$ for all glycolytic species involved in the model which are quite similar in chemical structure and molecular size. (We note that the assumption of equal diffusion coefficient for all species—among them the single- and double-phosphorylated species—is a strong simplification. For our purpose of qualitative modeling and principal study of the observed spatiotemporal dynamics in neutrophils, however, this is an adequate first step and the only one feasible, taking into consideration the lack of quantitative in vivo data on reaction kinetics and diffusive transport.) The modeling results are insensitive with respect to the numerical values of the diffusion coefficients within the range of factor of 5. Since the local concentrations of the glycolytic enzymes are assumed to be constant on the timescale of the observed phenomena, for these diffusive transport is not considered.

NUMERICAL METHODS

Computational modeling and simulation were done using several software packages. For simulation of the standard reaction-diffusion problem (1), we approximated the Laplacian operator using second-order finite differences and solved the discretized partial differential equation using the extrapolation integrator LIMEX (30). We assumed a rectangular domain $\Omega = [0, 20] \times [0, 7]$ and discretized in space with an equally distributed grid with a grid point spacing $\Delta x = 0.25$ μm. Visualizations were done using plotting functions implemented in MATLAB (The MathWorks, Natick, MA, www.mathworks.com).

For the computation in the realistic neutrophil geometry, we used the finite element library GASCOIGNE (31) with automatic grid generation using quadrilateral elements which has been developed for a posteriori error-controlled adaptive finite element simulations (32) in the Rannacher group at IWR Heidelberg, Germany. The visualization of the results were done using the visualization toolbox VISUSIMPLE (33). All computations were performed on PC with Intel Pentium IV, 3.6 GHz CPU, and 1 Gigabyte RAM.

RESULTS

In the following, we demonstrate that numerical simulations of our comprehensive model yield results consistent with most dynamic phenomena claimed by the Petty group based on fluorescence imaging observations. Therefore, provided some of the phenomena are real, the mechanism we propose could explain them at the systems' level with plausible and well-accepted biochemical concepts. Independent of the Petty observations, our study analyses the potential existence of such phenomena at the level of general feasibility.

Glycolysis model is capable of explaining NAD(P)H wave propagation

In Fig. 2, snapshots of numerical simulation results for the NAD(P)H wave propagation based on our glycolysis model are shown. For simplicity, we first assume a rectangular domain describing the shape of an adherent neutrophil and neglect the extension in z direction by projecting the neutrophil to the xy plane. Concerning the phenomenon of unidirectional wave propagation observed experimentally, this is a valid two-dimensional approximation for the moment and is further justified considering the flat elongated shape of an adherent neutrophil which is on average ~20 μm long, 7 μm wide, and 1–2 μm high (9).

For the ignition of glycolytic waves, a slightly increased glucose influx in the middle of the left boundary is applied. The presented simulation results show nearly the same wave properties, e.g., shape, velocity, and wave length, as the properties experimentally observed by Petty et al. (see Fig. 1). Waves have a longitudinal shape, always starting at the rear and propagating to the front of the cell with a velocity of ~27 μm/s, fully in the range of experimental results. After reaching the front of the cell wave, annihilation is observed and a new wave starts at the rear (see Fig. 2).

We conclude that glycolysis and its enzyme kinetics might give rise to NAD(P)H wave dynamics in neutrophils. However, in our model simulations we have ignited the waves artificially applying an increased glucose influx at a triggering point on the boundary. In the following, we remove this artificial boundary condition by considering a typical geometry of an adherent, polarized neutrophil.

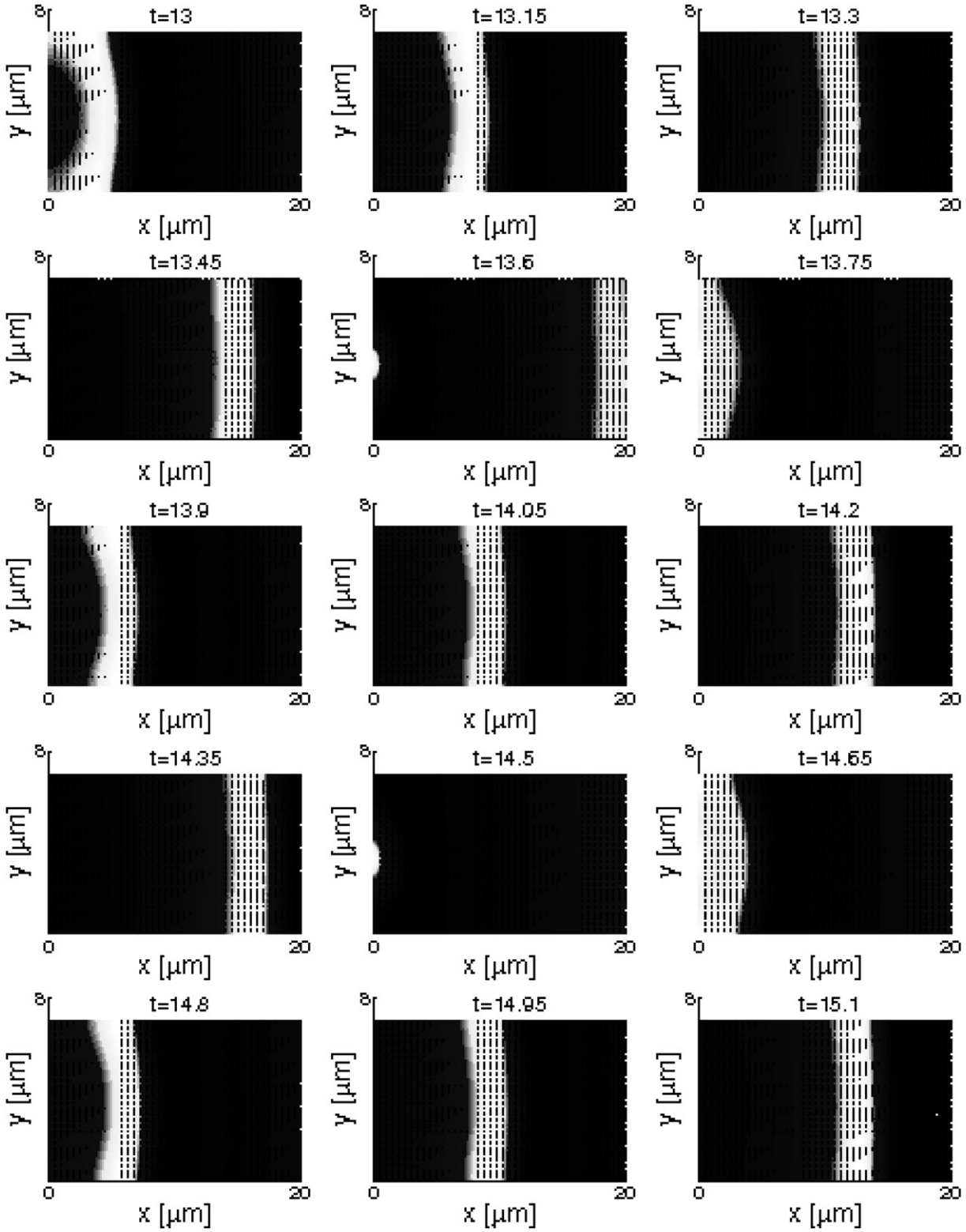

FIGURE 2 Snapshots of spatiotemporal simulation results for NAD(P)H wave propagation in neutrophils. Periodic wave trains with characteristics matching the experimentally observed ones. Initial conditions are provided in Table 4. We use [GLC] = 70 μmol in the middle of the left boundary, [GLC] = 5 μmol elsewhere. The simulations were performed using the code LIMEX (30).

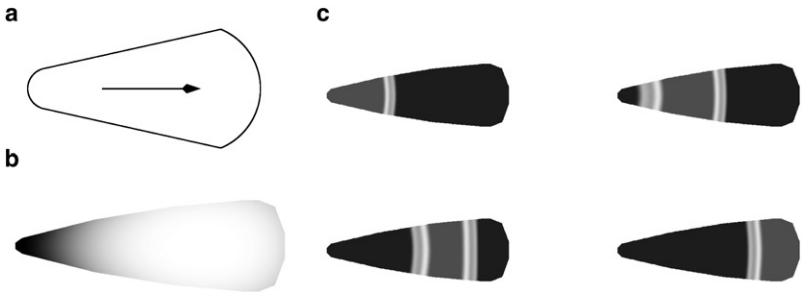

FIGURE 3 (*a*) Schematic view of a polarized, adherent neutrophil in a realistic geometry. The arrow marks the direction of polarization and migration. The front end is called the lamellipodium, while the rear end is called the uropod. (*b*) Visualization of intracellular glucose concentration caused by an uniform glucose influx in an asymmetrical geometry. Darker colors correspond to higher glucose concentration. The asymmetric glucose concentration initiates unidirectional metabolic wave propagation always starting at the rear (*left-hand side*). (*c*) Numerical simulation of unidirectional NAD(P)H wave propagation ignited by an asymmetric glucose concentration. A time series in steps of 0.2 s is shown. Solid representation corresponds to low, shaded representation to high NAD(P)H concentrations. For simulation we use the initial concentration [GLC] = 30 μmol. All other initial conditions are given in Table 4. The simulation were performed using the finite element toolbox GASCOIGNE (31).

Cell geometry may explain wave ignition and unidirectional wave propagation

To model a more realistic planar geometry (see Fig. 3 *a*), we consider a cell shape of an adherent polarized neutrophil with a wider front (lamellipodium) and a thinner rear (uropod). We assume, in contrast to the previous section, a uniform influx of glucose over the whole cell boundary and assume here glucose as diffusive with a diffusion constant $D_{\mathrm{GLC}} = 20\mu m^2/s$ and initial condition $[\mathrm{GLC}]_{\mathrm{init}} = 30\ \mu$mol. As a result of the asymmetric geometry of a polarized neutrophil, a higher glucose influx per volume is observed at the rear compared to the front (see Fig. 3 *b*), which results in autonomous triggering of unidirectionally propagating NAD(P)H waves (see Fig. 3 *c*).

This interpretation might be supported by experimental results. In spherical neutrophils, at the moment of adherence, spherical waves are observed by Petty et al. that are ignited at the point of adherence (34) and these only evolve to unidirectionally propagating longitudinal waves when the cell acquires the flat elongated and polarized shape. Our modeling result is important, since it provides novel insight. It demonstrates that the complexity of both ignition and unidirectionality of such NAD(P)H waves could be explained on the basis of very simple considerations, which concern cell geometry taking glucose membrane transport as a central regulatory process into account and coupling it to the dynamics of the glycolysis pathway. Independent of the Petty observations in neutrophils, such interplay between spatial effects and nonlinear enzyme kinetics may be an important general tool for the cell to generate a variety of different responses by utilizing one and the same metabolic or signaling pathway.

Enzyme translocation to the cell periphery upon activation may underlie NAD(P)H wave crossing and reflection

After activation of neutrophils with proinflammatory stimuli, Petty et al. observe two counter-propagating NAD(P)H-waves (3) which show the distinct characteristic behavior described in the introduction (boundary reflection and wave crossing). To investigate the possibility of such complex wave dynamics in the activated state, we consider intensity profile quantifications of the wave collision scenario which is available from experimental data published by Petty et al. After splitting of a single wave into two waves, they find a decrease by a factor of 2 in NAD(P)H fluorescence intensity (3), and during collision of the counter-propagating waves in the middle of the cell, the intensity profiles of both waves sum up.

Theoretical and experimental studies in other systems exhibiting chemical waves demonstrate the possible occurrence of wave splitting and reflection (35–37), but a splitting of intensities (wave amplitudes) is highly unusual. Therefore, we propose that such NAD(P)H wave crossing and reflection phenomena might be due to a three-dimensional effect with the waves passing each other in different planes in vertical direction. In Fig. 4 *a*, an approximation of the three-dimensional geometry of an adherent neutrophil is shown. For speedup of computations, exploiting a left-right symmetry, we use a cutting plane schematized in Fig. 4 *a* reducing our computational domain to two spatial dimensions. In activated neutrophils, enzyme translocation to the cell periphery has been found by Petty et al., e.g., for phosphofructokinase and hexokinase (15,38,39). We model this assuming a domain Ω_o of width $\Delta h = 0.5$ at the cell boundary with increased relative enzymes activity and an inner domain Ω_i with relatively decreased enzyme activity

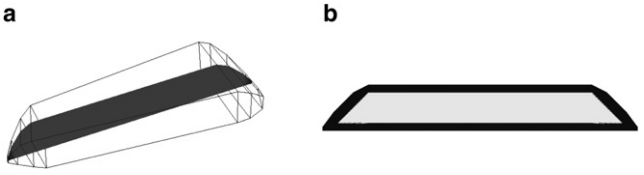

FIGURE 4 (*a*) Approximation of the three-dimensional geometry of a neutrophil with a total length of 20 μm, width of 7 μm, and height of 3 μm using polygons. Within the neutrophil the cutting plane is visualized (see text for details), which is used as a two-dimensional computational domain. (*b*) Visualization of the modeled enzyme translocation to the periphery after neutrophil activation with proinflammatory stimuli. Darker color corresponds to increased relative enzymes activity.

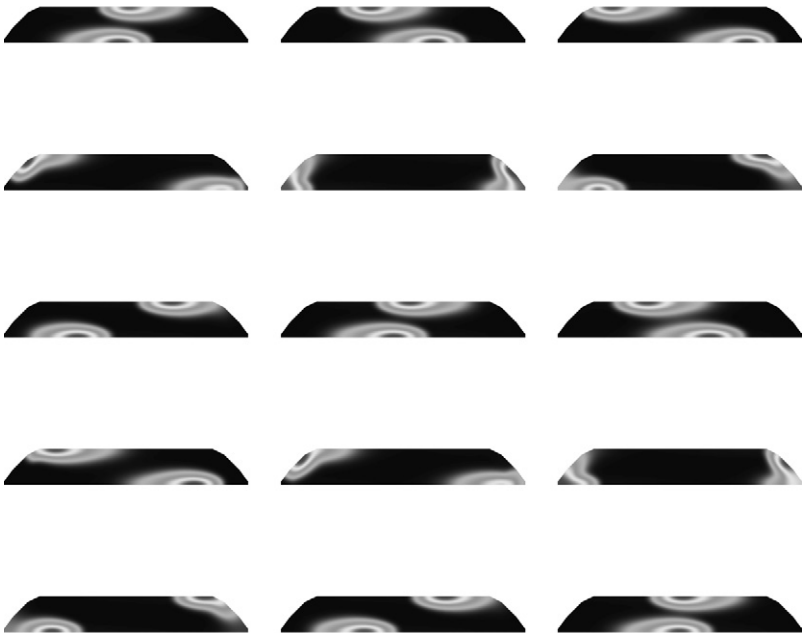

FIGURE 5 Numerical simulation of wave crossing caused by enzyme translocation observed in activated neutrophils. A time series in steps of 0.05 s is shown. Solid representation corresponds to low, shaded representation to high NAD(P)H concentrations. For simulation we use [GLC] = 4 μmol. Initial conditions for crossing initiation in Ω_o are [G6P] = 50 μmol and [FBP] = 0.1 μmol (see text for details). All other initial conditions are given in Table 4. The simulation were performed using the finite element toolbox GASCOIGNE (31).

modeled using a decreased $V_{pfk} = 1000$ μmol/s and $V_{hk} = 100$ μmol/s (see Fig. 4 *b*). We artificially initiate asymmetric wave propagation using increased initial concentration of metabolites in the middle of Ω_o (see Fig. 5 legend).

In Fig. 5, simulation results demonstrate wave crossing and reflection phenomena. It can be seen that both waves propagate near the membrane around the perimeter of the cell in a counterclockwise direction. When looking at the scenario from above or below through a microscope, this would appear as wave crossing and wave reflection behavior experimentally observed by Petty et al. The corresponding splitting of intensities (amplitudes) in our model simulations is shown in Fig. 6.

Dynamically regulated glucose influx could explain NAD(P)H oscillations consistent with wave propagation

Since temporal oscillations of NAD(P)H are observed in fluorimetric whole-cell measurements by Petty et al., we consider a potential mechanism giving rise to such oscillations in addition to the wave phenomena. The timescale of the oscillations (20 s period in the nonactivated and 10 s in the activated state) is different from the wave dynamics (~600 ms for crossing a cell of 20-μm length). Integrating wave intensities from our numerical simulations over the whole cell does not result in temporal oscillations with comparable periods.

However, in a previous article, we demonstrated how to analyze possible cellular signaling routes using mathematical optimal control techniques (40), which have turned out to be useful for studying self-organized dynamics and pattern formation in biological systems (41–43). We applied this method to analyze a potential dependence of glycolytic NAD(P)H-oscillations on dynamically varying input stimuli, among them a periodic glucose influx (40). We found that a periodic forcing of the glucose influx results in the experimentally observed harmonic oscillations of NAD(P)H. Interestingly, as a result of the mathematical solution of our model-based optimal control problem, the periodic glucose influx rate and the induced NAD(P)H oscillations have a specific phase difference. This is the same phase shift observed experimentally between NAD(P)H and Ca^{2+} (5) by Petty et al., inspiring us to suggest a possible regulatory link among NAD(P)H-production, Ca^{2+}-signaling, and glucose membrane transport.

Observations by Petty et al. show that the phase difference between calcium and NAD(P)H oscillations remains constant over time, even after activation and switching from a 20 s to a 10 s period, a phenomenon which is called phase-locking. This would strongly support the hypothesis of a direct mutual coupling between both oscillators. Kummer et al. (13) hypothesized that metabolism might be able to drive Ca^{2+} oscillations, but they do not say how. Our modeling results provide additional evidence for a potential driving of metabolism by calcium-induced and dynamically regulated glucose influx, possibly via calcium activation of glucose transporters (GLUT) in the plasma membrane. This regulation may include translocation of glucose transporters to the membrane (44) or their activation by (for example) phosphorylation, which has been observed in monocyte-macrophage cell lines (45), and this will cause a further phase delay between both oscillators and could result in the experimentally observed phase shift. This hypothesis and the mutual coupling of metabolism and calcium signaling will be discussed in detail in the next section.

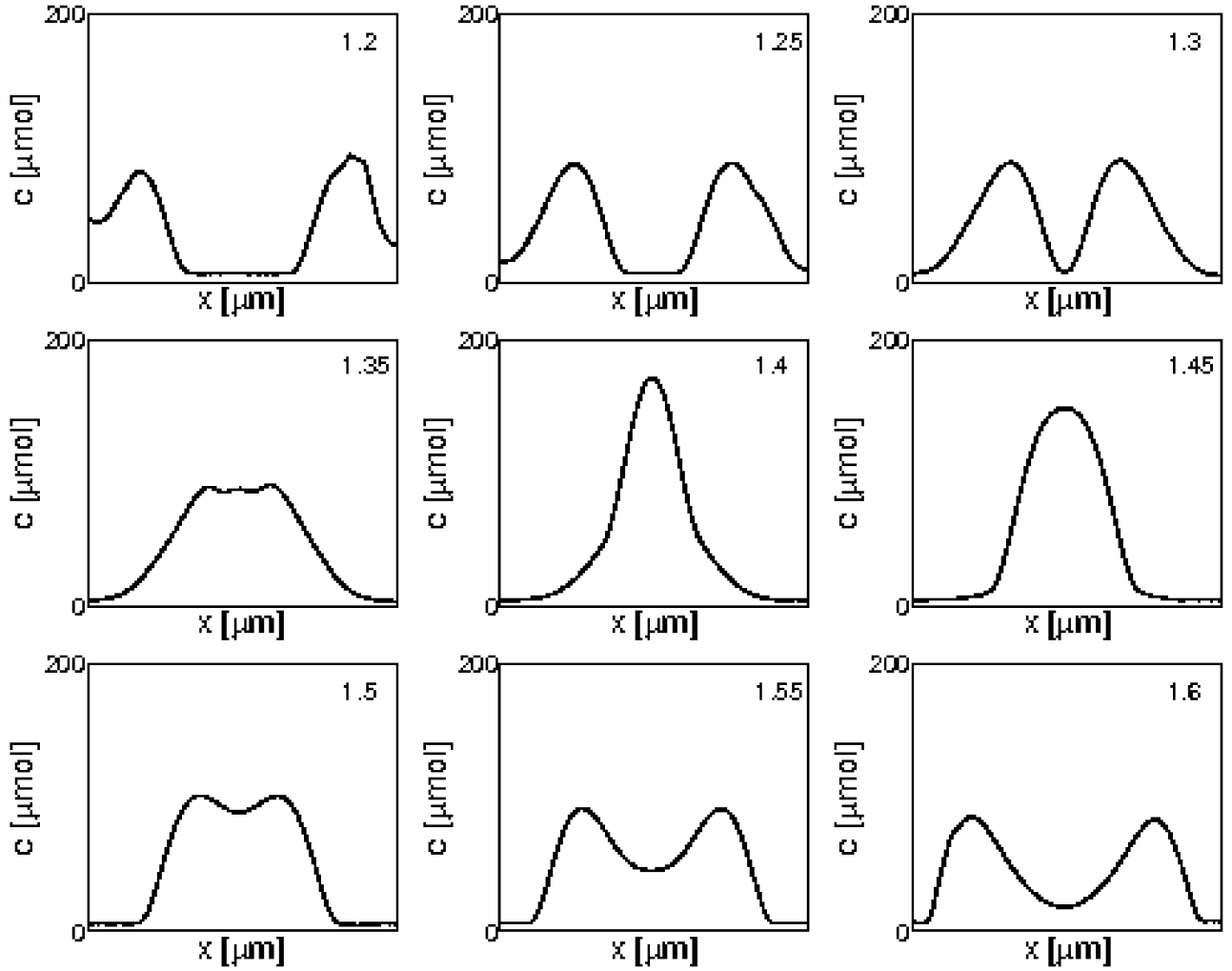

FIGURE 6 Intensity profiles obtained looking at the wave-crossing results presented in Fig. 5 from a vertical perspective. These profiles coincide with experimental observations (Fig. 2 in (3)).

Feedback coupling between NAD(P)H and calcium dynamics through cADPR could explain switching between different oscillation periods upon neutrophil activation

It has been claimed that neutrophil activation by chemoattractants or proinflammatory cytokines is linked to an activation of the hexose-monophosphate shunt (HMS) (see (13–15,46) and references therein)). To analyze whether such an activation mechanism would be able to explain a period switching in calcium and NAD(P)H oscillations observed experimentally (13), we added a calcium model to our spatiotemporal model of glycolysis.

It has been discussed that cADPR-gated calcium entry plays an important role during neutrophil chemotaxis (24). cADPR is synthesized from NAD^+ by the enzyme CD38 and is known to trigger calcium release from intracellular stores (47,48). Incorporating this into our model (see Modeling), we find, in addition to an underlying wave propagation, a switching behavior of the oscillation period upon activation of the HMS in numerical simulation (see Fig. 7) and therefore propose a potential feedback-coupling mechanism between calcium and metabolic dynamics. This mechanism contains, as key ingredients, the calcium-controlled glucose influx and a calcium ER-channel gating controlled by cADPR synthesized from NAD^+—which are plausible assumptions based on literature knowledge (47,49,50).

The details of its regulation are not known right now. Perhaps a calcium binding and activation of enzymes responsible for phosphorylation or other regulations of GLUT translocation and activity might be involved. A more detailed investigation of the interplay of calcium and glucose transport proposed in our theoretical study may be part of future research.

Using the fully coupled model, temporal oscillations together with spatiotemporal wave dynamics can simultaneously be explained. In Fig. 7 of Kummer et al. (13) showing simultaneous NAD(P)H and calcium oscillations and its period switching after activation, it can be seen that an activation signal may only be transmitted after crossing a minimum of the NAD(P)H oscillation. Because of the fact that in

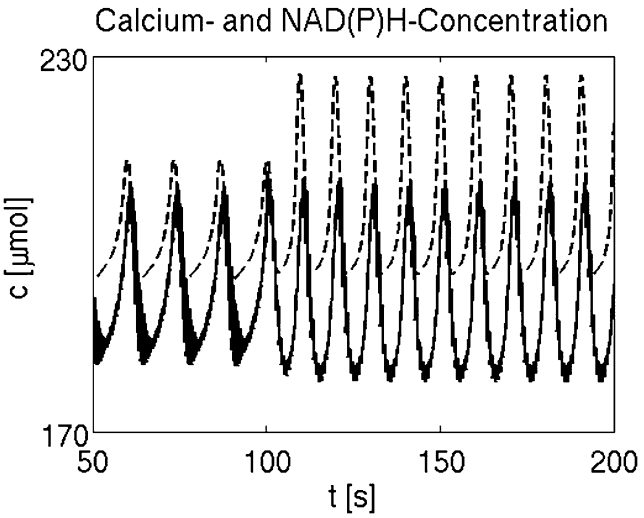

FIGURE 7 Simultaneous NAD(P)H and Ca^{2+} oscillations resulting from integration over the whole cell in each time point of the numerical simulation. This is a result of the underlying NAD(P)H wave propagation with oscillating amplitudes driven by Ca^{2+}-activated periodic glucose influx into the cell (see text). At $t = 100$ the HMS is switched on from $k_{hms} = 0.01$ to $k_{hms} = 2$. After $t = 100$, the HMS becomes activated, and NADPH also contributes strongly to the NAD(P)H signal (~50%). Dashed lines correspond to Ca^{2+} oscillations. Initial conditions are given in Table 4 and we use [GLC] = 80 μmol in the middle of the left boundary for triggering of the waves.

a minimum of the NAD(P)H oscillations the cellular NAD^+ concentration is maximal, this results in an increasing cADPR concentration followed by a stimulated calcium efflux from the intracellular stores in our model. Finally, increased calcium concentration activates glucose transport and thereby results in a mutual stabilization of both oscillators. During neutrophil activation, which includes an activation of the HMS, a decreased substrate flux through the glycolysis pathway results in an accelerated increase of NAD^+ concentration. This stimulates faster cADPR production and a calcium efflux via ryanodine receptors is forced. Using a calcium-dependent glucose influx, a feedback coupling on the metabolism stabilizes both oscillators and a frequency increase is observed.

SUMMARY AND DISCUSSION

In our study, we have applied spatiotemporal modeling to propose a possible biochemical mechanism which, in principle, could explain controversial metabolic wave and oscillation phenomena in neutrophils and their coupling to calcium signaling claimed by Petty et al. on the basis of high-speed fluorescence imaging observations. For this purpose, we adapted and modified a previously published glycolysis model (13) and extended it to include diffusive transport of glycolytic metabolites as well as regulated glucose transport over the plasma membrane. The model of Kummer et al. assumes the oscillations of NAD(P)H to be caused by autonomous oscillatory dynamics of the glycolysis pathway. They adapt the model parameters to result in the experimentally observed range of a 20-s period (nonactivated state) and 10-s period (activated state). However, they do not make an attempt to explain the coexistence of NAD(P)H-oscillations, metabolic waves and phase-locked calcium oscillations. Adding diffusion terms to the Kummer model does not yield the coexistence of any of these phenomena. Therefore, the Kummer model is not consistent with the holistic system behavior. We demonstrate that our model is capable of producing NAD(P)H waves with nearly the same characteristics (e.g., shape, velocity, and wave length) as those published by the Petty group. According to our spatiotemporal modeling results in a realistic cell morphology, we show that the initiation of NAD(P)H-waves at the uropod could be explained by geometric reasoning. Assuming a spatially uniform glucose influx over the plasma membrane, in our numerical simulations unidirectionally propagating NAD(P)H waves occur starting at the rear obviously caused by a higher glucose per volume influx at the thinner end than at the wider front of the cell. Our model is consistent with most experimental observations published by Petty et al., e.g., boundary reflection and wave-crossing behavior in activated neutrophils after incorporating enzyme translocation to the cell periphery upon proinflammatory activation.

We hypothesize a periodic glucose influx potentially driving the metabolic oscillation and a feedback-coupling to calcium signaling via cADPR synthesis from NAD^+ and cADPR gating of calcium entry from intracellular stores. We demonstrate that, assuming activation of the hexose-monophosphate shunt, this mechanisms would be able to explain a switching of oscillation periods of both NAD(P)H and calcium from ~20 s to 10 s as claimed by Petty et al. after proinflammatory activation of neutrophils. The assumption of a forcing of glucose influx by calcium is further motivated by the knowledge that glucose transport in neutrophils, as related to the activation state, is dynamically regulated (26), and the fact that calcium seems to be involved in this regulation (27).

We concluded from these results that a plausible underlying mechanism could be a Ca^{2+}-dependent periodic activation of glucose transport over the plasma membrane. Its regulation may rely on fusion of intracellular vesicles containing GLUT transporters with the plasma membrane (44) or phosphorylation of glucose transporters GLUT (45).

A dependence on calcium of the regulation of glucose membrane transport in neutrophils activated by chemotactic peptides has been concluded from an experimental study (51) where the authors apply a calcium ionophore, which increases the permeability of biological membranes with high selectivity for divalent cations like calcium (52). Since neutrophil activation also corresponds to changes in metabolic activity (13–15), this further confirms an effect of calcium signaling on metabolism via regulation of glucose membrane transport.

Facilitated transport of glucose across the plasma membrane is known to be an important part of the regulation

of metabolic activity. Therefore, it has been studied in detail (see (53) for a review of metabolic regulation of glucose transport). Interestingly, in activated neutrophils increased glucose levels are measured experimentally (26,44) and thus glucose transport rate seems to be regulated with respect to the state of activation. Glucose transport into cells is mediated by a family of homologous glycoprotein molecules, called GLUT. In neutrophils, the glucose transporter GLUT1 is found (44). For these GLUT1, a dependence of the glucose transport rate on calcium has been found (53). A calcium-dependent increase of glucose uptake via the glucose transporter GLUT1 has been observed in a human megakaryocytic cell line (54), rat liver cell line (55), and rat epithelial cells (56) via a yet unknown mechanism.

Independent from the Petty results, oscillatory processes in neutrophils have also been observed by other groups. The first report about oscillatory behavior in neutrophils by Jäger et al. (57) states oscillations in membrane potential. Calcium oscillations with an ~10 s periodicity applying proinflammatory agents have been measured by several groups (58–61). Periodic behavior in filamentous actin content has been found (62–64), and respiratory burst (65) and cellular shape change (66,67) has been experimentally observed.

Our spatiotemporal modeling study will hopefully stimulate comprehensive experimental efforts to fully reveal the existence and a potentially underlying mechanism of any kind of wave and oscillation phenomena in neutrophils and promote their mechanistic elucidation.

The authors thank The Freiburg Initiative for Systems Biology as a part of the German FORSYS systems biology initiative funded by the German Federal Ministry of Research and Education (Bundesministerium für Bildung und Forschung, i.e., BMBF).

O.S. thanks the "International Graduate College 710: Modeling, Simulation and Optimization."

REFERENCES

1. Janeway, C. 2004. Immunobiology, 6th Ed. Garland Science, London.
2. Burg, N. D., and M. H. Pillinger. 2001. The neutrophil: function and regulation in innate and humoral immunity. *Clin. Immunol.* 99: 7–17.
3. Petty, H. R., and A. L. Kindzelskii. 2001. Dissipative metabolic patterns respond during neutrophil transmembrane signaling. *Proc. Natl. Acad. Sci. USA.* 98:3145–3149.
4. Petty, H. R. 2006. Spatiotemporal chemical dynamics in living cells: from information trafficking to cell physiology. *Biosystems.* 83:217–224.
5. Petty, H. R. 2000. Oscillatory signals in migrating neutrophils: effects of time-varying chemical and electric fields. *In* Self-Organized Biological Dynamics & Nonlinear Control. J. Walleczek, editor. Cambridge University Press, Cambridge.
6. Adachi, Y., A. L. Kindzelskii, N. Ohno, T. Yadomae, and H. R. Petty. 1999. Amplitude and frequency modulation of metabolic signals in leukocytes: synergistic role of IFN-γ in IL-6- and IL-2-mediated cell activation. *J. Immunol.* 163:4367–4374.
7. Petty, H. R. 2001. Neutrophil oscillations: temporal and spatiotemporal aspects of cell behavior. *Immunol. Res.* 23:85–94.
8. Petty, H. R. 2004. Applications of high speed microscopy in biomedical research. *Opt. Photonics News.* 1:34–40.
9. Petty, H. R., R. G. Worth, and A. L. Kindzelskii. 2000. Imaging sustained dissipative patterns in the metabolism of individual living cells. *Phys. Rev. Lett.* 84:2754–2757.
10. Kindzelskii, A. L., and H. R. Petty. 2003. Intracellular calcium waves accompany neutrophil polarization, formylmethionyl leucylphenylalanine stimulation, and phagocytosis: a high speed microscopy study. *J. Immunol.* 170:64–72.
11. Hillson, E. J., and M. B. Hallett. 2007. Localized and rapid Ca^{2+} micro–events in human neutrophils: Conventional Ca^{2+} puffs and global waves without peripheral-restriction or wave cycling. *Cell Calcium.* 41:525–536.
12. Reble, C. 2007. Experimental and theoretical investigations of dissipative structures in living human immune cells. Diploma thesis. University of Heidelberg, Heidelberg, Germany.
13. Kummer, U., J. Zobeley, J. C. Brasen, R. Fahmy, A. L. Kindzelskii, et al. 2007. Elevated glucose concentration promote receptor-independent activation of adherent human neutrophils: an experimental and computational approach. *Biophys. J.* 92:2597–2607.
14. Roos, D., and A. J. M. Balm. 1980. The oxidative metabolism of monocytes. *In* The Reticuloendothelial System: A Comprehensive Treatise. A. J. Sbarra and R. R. Strauss, editors. Plenum Press, New York.
15. Kindzelskii, A. L., J. B. Huang, T. Chaiworapongsa, R. M. Fahmy, Y. M. Kim, et al. 2002. Pregnancy alters glucose-6-phosphate dehydrogenase trafficking, cell metabolism, and oxidant release of maternal neutrophils. *J. Clin. Invest.* 110:1801–1811.
16. Westermark, P. O., and A. Lansner. 2003. A model of phosphofructokinase and glycolytic oscillations in the pancreatic β-cells. *Biophys. J.* 85:126–139.
17. Hofmeyr, J. -H., and A. Cornish-Bowden. 1997. The reversible Hill equation: how to incorporate cooperative enzymes into metabolic models. *Comput. Appl. Biosci.* 13:377–385.
18. Shimizu, T., J. C. Parker, H. Najafi, and F. M. Matschinsky. 1988. Control of glucose metabolism in pancreatic β-cells by glucokinase, hexokinase, and phosphofructokinase. Model study with cell lines derived from β-cells. *Diabetes.* 37:1524–1530.
19. Trus, M., H. Warner, and F. Matschinsky. 1980. Effects of glucose on insulin release and on intermediary metabolism of isolated perifused pancreatic islets from fed and fasted rats. *Diabetes.* 29:1–14.
20. Li, Y. X., and J. Rinzel. 1994. Equations for $InsP_3$ receptor-mediated $[Ca^{2+}]_i$ oscillations derived from a detailed kinetic model: a Hodgkin-Huxley like formalism. *J. Theor. Biol.* 166:461–473.
21. Pettit, E. J., and M. B. Hallett. 1995. Early Ca^{2+} signaling events in neutrophils detected by rapid confocal laser scanning. *Exp. Cell Res.* 310:445–448.
22. Pettit, E. J., and M. B. Hallett. 2000. Nonuniform distribution of Ca^{2+} uptake sites within human neutrophils. *Biochem. Biophys. Res. Commun.* 279:337–340.
23. Hauser, C. J., K. B. Kannan, E. A. Deitch, and K. Itagaki. 2005. Nonspecific effects of 4-chloro-m-cresol may cause calcium flux and respiratory burst in human neutrophils. *Biochem. Biophys. Res. Commun.* 336:1087–1095.
24. Partida-Sanchez, S., A. Gasser, R. Fliegert, C. C. Siebrands, W. Dammermann, et al. 2007. Chemotaxis of mouse bone marrow neutrophils and dendritic cells is controlled by ADP-ribose, the major product generated by the CD38 enzyme reaction. *J. Immunol.* 179: 7827–7839.
25. Partida-Sanchez, S., D. A. Cockayne, S. Monard, E. L. Jacobson, N. Oppenheimer, et al. 2001. Cyclic ADP-ribose production by CD38 regulates intracellular calcium release, extracellular calcium influx and chemotaxis in neutrophils and is required for bacterial clearance in vivo. *Nat. Med.* 7:1209–1216.
26. Tan, A. S., N. Ahmed, and M. V. Berridge. 1998. Acute regulation of glucose transport after activation of human peripheral blood neutrophils by phorbol myristrate acetate, fMLP, and granulocyte-macrophage colony-stimulating factor. *Blood.* 91:649–655.

27. O'Flaherty, J. T., S. Cousart, C. L. Swendsen, L. R. DeChatelet, D. A. Bass, et al. 1981. Role of Ca^{2+} and Mg^{2+} in neutrophil hexose transport. *Biochim. Biophys. Acta.* 640:223–230.

28. Atkins, P. W. 1990. Physical Chemistry, 4th Ed. Oxford University Press, Oxford.

29. Luby-Phelps, K. 2000. Cytoarchitecture and physical properties of cytoplasm: volume, viscosity, diffusion, intracellular surface area. *Int. Rev. Cytol.* 192:189–221.

30. Deuflhard, P., and U. Nowak. 1987. Extrapolation integrators for quasilinear implicit ODEs. *In* Large Scale Scientific Computing. P. Deuflhard and B. Engquist, editors. Birkhäuser, Boston, Basel, Stuttgart.

31. Becker, R., M. Braak, T. Dunne, D. Meidner, T. Richter, et al. GASCOIGNE, a C++ numerics library for scientific computing, http://www.gascoigne.de/.

32. Rannacher, R. 2001. Adaptive Galerkin finite element methods for partial differential equations. *J. Comput. Appl. Math.* 128:169–178.

33. Becker, R., T. Dunne, and D. Meidner, VisuSimple, an interactive visualization program for 2D- and 3D-data, http://dunne.uni-hd.de/VisuSimple/.

34. Petty, H. R., and A. L. Kindzelskii. 2000. High-speed imaging of sustained metabolic target patterns in living neutrophils during adherence. *J. Phys. Chem. B.* 104:10952–10955.

35. Meinhardt, H. 1982. Models of Biological Pattern Formation. Academic Press, London.

36. Munuzuri, A. P., V. Perez-Villar, and M. Markus. 1997. Splitting of autowaves in an active medium. *Phys. Rev. Lett.* 79:1941–1944.

37. Petrov, V., S. K. Scott, and K. Showalter. 1994. Excitability, wave reflection, and wave splitting in a cubic autocatalysis reaction-diffusion system. *Philos. Trans. R. Soc. Lond. A.* 347:631–642.

38. Kindzelskii, A. L., A. J. Clark, J. Espinoza, N. Maeda, Y. Aratani, et al. 2006. Myeloperoxidase accumulates at the neutrophil surface and enhances cell metabolism and oxidant release during pregnancy. *Eur. J. Immunol.* 36:1–10.

39. Huang, J. -B., A. L. Kindzelskii, and H. R. Petty. 2002. Hexokinase translocation during neutrophil activation, chemotaxis, and phagocytosis: disruption by cytochalasin D, dexamethasone, and indomethicin. *Cell. Immunol.* 218:95–106.

40. Slaby, O., S. Sager, O. S. Shaik, U. Kummer, and D. Lebiedz. 2007. Optimal control of self-organized dynamics in cellular signal transduction. *Math. Comp. Model. Dyn.* 13:487–502.

41. Lebiedz, D., and U. Brandt-Pollmann. 2003. Manipulation of self aggregation patterns and waves in a reaction-diffusion-system by optimal boundary control strategies. *Phys. Rev. Lett.* 91:208301.

42. Lebiedz, D., S. Sager, H. -G. Bock, and P. Lebiedz. 2005. Annihilation of limit cycle oscillations by identification of critical phase resetting stimuli via mixed-integer optimal control methods. *Phys. Rev. Lett.* 95:108303.

43. Lebiedz, D., and H. Maurer. 2004. External optimal control of self-organization dynamics in a chemotaxis reaction diffusion system. *Syst. Biol.* 1:222–229.

44. Schuster, D. P., S. L. Brody, Z. Zhou, M. Bernstein, R. Arch, et al. 2007. Regulation of lipopolysaccaride-induced increases in neutrophil glucose uptake. *Am. J. Physiol. Lung Cell. Mol. Physiol.* 292:L845–L851.

45. Ahmed, N., M. Kansara, and V. Berridge. 1997. Acute regulation of glucose transport in a monocyte-macrophage cell line: GLUT-3 affinity for glucose is enhanced during the respiratory burst. *Biochem. J.* 327:369–375.

46. Huang, J. B., J. Espinozy, R. Romero, and H. R. Petty. 2006. Apparent role of dynein in glucose-6-phosphate dehydrogenase trafficking in neutrophils from pregnant women. *Metab. Clin. Exp.* 55:279–281.

47. Lee, H. C. 2002. Cyclic ADP-ribose and NAADP. Springer, New York, Berlin, Heidelberg.

48. Galione, A., and G. C. Churchill. 2002. Interactions between calcium release pathways: multiple messengers and multiple stores. *Cell Calcium.* 32:343–354.

49. Schuster, F., and F. E. Lund. 2004. Structure and enzymology of ADP-ribosyl cyclases: conserved enzymes that produce multiple calcium mobilizing metabolites. *Curr. Mol. Med.* 4:249–261.

50. Lee, H. C. 1997. Mechanisms of calcium signaling by cyclic ADP-ribose and NAADP. *Physiol. Rev.* 77:1133–1164.

51. Okuno, Y., and J. Gliemann. 1988. Effect of chemotactic factors on hexose transport in polymorphonuclear leucocytes. *Biochim. Biophys. Acta.* 941:157–164.

52. Akerman, K. E. O., M. O. Proudlove, and A. L. Moore. 1983. Evidence for a Ca^{2+} gradient across the plasma membrane of wheat protoplasts. *Biochem. Biophys. Res. Commun.* 113:171–177.

53. Ismail-Beigi, F. 1993. Metabolic regulation of glucose transport. *J. Membr. Biol.* 135:1–10.

54. Maraldi, T., M. Rugolo, D. Fiorentini, L. Landi, and G. Hakim. 2006. Glucose transport activation in human hematopoietic cells M07e is modulated by cytosolic calcium and calmodulin. *Cell Calcium.* 40:373–381.

55. Mitani, Y., A. Behrooz, G. R. Dubyak, and F. Ismail-Beigi. 1995. Stimulation of GLUT-1 glucose transporter expression in response to exposure to calcium ionophore A-23187. *Am. J. Physiol. Cell Physiol.* 269:C1228–C1234.

56. Quintanilla, R. A., O. H. Porras, J. Castro, and L. F. Barros. 2000. Cytosolic [Ca^{2+}] modulates basal GLUT1 activity and plays a permissive role in its activation by metabolic stress and insulin in rat epithelial cells. *Cell Calcium.* 28:97–105.

57. Jäger, U., H. Gruler, and B. Bültmann. 1988. Morphological changes and membrane potential of human granulocytes under influence of chemotactic peptide and/or Echo-Virus, Type 9. *J. Mol. Med.* 66:434–436.

58. Davies, E. V., A. K. Campell, and M. B. Hallett. 1994. Ca^{2+} oscillations in neutrophils triggered by immune complexes result from Ca^{2+} influx. *Immunology.* 82:57–62.

59. Jacob, R. 1990. Imaging cytoplasmic free calcium in histamine stimulated endothelial cells and in fMet-Leu-Phe stimulated neutrophils. *Cell Calcium.* 11:241–249.

60. Jaconi, M. E. E., R. W. Rives, W. Schlegel, C. B. Wollheim, D. Pittet, et al. 1988. Spontaneous and chemoattractant-induced oscillations of cytosolic adherent human neutrophils. *J. Biol. Chem.* 263:10557–10560.

61. Rotnes, J. S., and J. A. Rottingen. 1994. Quantitative analysis of cytosolic free calcium oscillations in neutrophils by mathematical modeling. *Cell Calcium.* 15:467–482.

62. Omann, G. M., M. M. Porasik, and L. A. Skalar. 1989. Oscillating actin polymerization/depolymerization responses in human polymorphonuclear leukocytes. *J. Biol. Chem.* 264:16355–16358.

63. Rengan, R., and G. M. Omann. 1999. Regulation of oscillations in filamentous actin content in polymorphonuclear leukocytes stimulated with leukotriene B_4 and platelet-activating factor. *Biochem. Biophys. Res. Commun.* 262:479–486.

64. Wymann, M. P., P. Kernen, T. Bengtsson, T. Andersson, M. Baggiolini, et al. 1990. Corresponding oscillations in neutrophil shape and filamentous actin content. *Biochem. Biophys. Res. Commun.* 265:619–622.

65. Wymann, M. P., P. Kernen, D. A. Deranleau, and M. Baggiolini. 1989. Respiratory burst oscillations in human neutrophils and their correlation with fluctuations in apparent cell shape. *J. Biol. Chem.* 264:15829–15834.

66. Ehrengruber, M. U., P. Boquet, T. D. Coates, and D. A. Deranleau. 1995. ADP-ribosylation of Rho enhances actin polymerization-coupled shape oscillations in human neutrophils. *FEBS Lett.* 372: 161–164.

67. Ehrengruber, M. U., D. A. Deranleau, and T. D. Coates. 1996. Shape oscillations of human neutrophil leukocytes: characterization and relationship to cell motility. *J. Exp. Biol.* 199:741–747.